Water Molecules Coupled to the Redox-Active Tyrosine Y_D in Photosystem II as Detected by FTIR Spectroscopy†

Ryouta Takahashi,‡ Miwa Sugiura,§ and Takumi Noguchi*,‡

Institute of Materials Science, University of Tsukuba, Tsukuba, Ibaraki 305-8573, Japan, and Department of Plant Biosciences, School of Life and Environmental Sciences, Osaka Prefecture University, 1-1 Gakuen-cho, Sakai, Osaka, 599-8531 Japan

Received August 28, 2007; Revised Manuscript Received October 2, 2007

ABSTRACT: The redox-active tyrosine Y_D (D2-Tyr160) in photosystem II (PSII) serves as a side-path electron donor to P680. When Y_D is oxidized, a proton is released from phenolic OH, and a neutral radical $Y_D^\bullet$ is formed. A hydrogen bond network around Y_D must be deeply involved in the mechanism of the Y_D reaction. In this study, we have detected water molecules structurally coupled to Y_D by means of Fourier transform infrared (FTIR) spectroscopy. Light-induced $Y_D^\bullet/Y_D$ FTIR difference spectrum of a hydrated film of the PSII core complexes from *Thermosynechococcus elongatus* showed major signals at 3636(−)/3617(+) and 3594(+)/3585(−) cm^{-1} in the weakly hydrogen bonded OH stretching region. These peaks downshifted by 11−12 cm^{-1} upon $H_2{}^{18}O$ substitution and almost disappeared upon H/D exchange, and hence, they were definitely assigned to the water OH vibrations. Small intramolecular couplings of 3−6 cm^{-1} estimated from the OH frequencies of residual HOD species in a deuterated film indicate that these OH signals arise from two different water molecules that have significantly asymmetric hydrogen bond structures. Similar OH signals were observed in PSII-enriched membranes from spinach, suggesting that two water molecules commonly exist near Y_D irrespective of biological species. These water molecules are coupled to Y_D most probably through a hydrogen bond network or one of them possibly interacts directly with Y_D, and thus, they may play crucial roles in the Y_D reaction by forming a proton-transfer pathway and tuning the redox potential of Y_D.

The redox-active tyrosine Y_D[1] (D2-Tyr160) in photosystem II (PSII) serves as an electron donor to the special-pair chlorophyll P680. When Y_D is oxidized, a proton is released from phenolic OH, and a neutral radical $Y_D^\bullet$ is produced (*1*−*5*), reflecting a extremely low pK_a of −2 for the cation radical (*6*). While another redox-active tyrosine Y_Z (D1-Tyr161), which is symmetrically located in the PSII complex, functions in a main electron-transfer pathway from the oxygen-evolving Mn cluster to P680, Y_D is related to peripheral electron-transfer processes involving P680 and the Mn cluster (*1*−*5*). Y_D may play physiological roles in preventing over-reduction of the Mn cluster to maintain stable valence states and tuning the $P680^+$ property electrostatically or through a hydrogen bond network (*3*, *7*). The redox potential of $Y_D^\bullet/Y_D$ has been estimated to be +0.72−0.76 mV (*8*, *9*), which is much lower than that of $Y_Z^\bullet/Y_Z$ (approximately +1 V) (*1*). The reason for the low redox potential of Y_D remains unclarified. Recent quantum chemical calculations suggested that the hydrogen bond network around Y_D plays a crucial role in determining the redox potential (*10*).

The protein structure around Y_D has been revealed by X-ray crystallographic studies of PSII core complexes from *Thermosynechococcus elongatus* at 3.0−3.5 Å resolution (*11*, *12*). The side chain of D2-His189 is located at a hydrogen bonding distance to the phenolic OH of Y_D, and that of D2-Gln164 is also in close vicinity. The X-ray structures also showed a hydrogen bond network involving D2-Arg294, CP47-Glu364, and D2-Asn292 in addition to D2-His189 and D2-Gln164, while no water molecules have been resolved so far. Exchangeable protons near $Y_D^\bullet$ have been detected by ENDOR and ESEEM spectroscopies (*13*−*19*). Direct interaction with D2-His189 has been revealed by ENDOR (*17*, *20*), high-field EPR (*21*), and FTIR (*22*) measurements in combination with specific ^{15}N isotope substitution of histidines or site-directed mutation of D2-His189.

It has been thought that the proton released from Y_D remains in the vicinity of Y_D (*2*, *3*). D2-H189 or a nearby residue may accept the proton, or it can be shared within a hydrogen bond network (*2*, *3*, *23*). FTIR measurements by Hienerwadel et al. (*23*), however, detected protons released from PSII proteins upon Y_D oxidation as changes in buffer bands, although they could not conclude whether the proton originates from Y_D or arises from residues at the protein surface due to an electrostatic effect. Thus, the fate of the proton released upon Y_D oxidation has not been clarified yet. It is essential to identify the proton-transfer pathway

† This study was supported by Grants-in-Aid for Scientific Research (17GS0314 and 18570145 to T.N. and 18770116 to M.S.) from the Ministry of Education, Science, Sports, Culture and Technology, and a grant from Nissan Science Foundation (to M.S).

* To whom correspondence should be addressed. Tel.: +81-29-853-5126; fax: +81-29-853-4490; e-mail: tnoguchi@ims.tsukuba.ac.jp.

‡ University of Tsukuba.

§ Osaka Prefecture University.

[1] Abbreviations: DM, *n*-dodecyl-*β*-D-maltoside; FTIR, Fourier transform infrared ; Mes, 2-(*N*-morpholino)ethanesulfonic acid; PSII, photosystem II; P680, the special pair chlorophyll of photosystem II; Y_D, redox-active tyrosine on the D2 protein; Y_Z, redox-active tyrosine on the D1 protein.

10.1021/bi701752d CCC: $37.00
Published on Web 11/13/2007

and the protonation states of residues involved in this pathway to answer this question.

In this study, we have for the first time detected water molecules structurally coupled to Y_D by means of light-induced FTIR difference spectroscopy. This technique has been applied to various redox cofactors in PSII to study their reactions and couplings with surrounding molecules (*24*). $Y_D^{\bullet}/Y_D$ FTIR spectra have been reported only in the mid-frequency region (1800−1000 cm^{-1}) thus far (*22*, *23*, *25*−*27*). Here, we have measured the high-frequency region (3700−3500 cm^{-1}), where OH stretching vibrations of water occur (*28*−*31*), using moderately hydrated films of PSII preparations from *T. elongatus* and spinach. Two water molecules, probably involved in the hydrogen bond network around Y_D, were identified. These water molecules may play a crucial role in the mechanism of Y_D oxidation and a concomitant proton-transfer reaction.

MATERIALS AND METHODS

PSII core complexes of *T. elongatus*, in which the carboxyl terminus of the CP43 subunit was genetically His-tagged, were purified as previously described (*32*). Mn depletion was performed by 10 mM NH_2OH treatment for 30 min at room temperature (*32*). PSII-enriched membranes of spinach were prepared as reported previously (*33*), and Mn depletion was performed by 1 M Tris-HCl (pH 8.5) treatment.

For $Y_D^{\bullet}/Y_D$ FTIR measurements of *T. elongatus* core complexes, 5 μL of a suspension of the Mn-depleted PSII core complexes (3.0 mg Chl/mL) in a pH 6.0 Mes buffer (10 mM Mes, 5 mM NaCl, and 0.06% DM) was mixed with 0.5 μL of 200 mM sodium formate, 1 μL of 20 mM potassium ferricyanide, and 1 μL of 20 mM potassium ferrocyanide. The addition of sodium formate was omitted for the measurements without formate treatment. For measurements of spinach PSII, 5 μL of Mn-depleted PSII-enriched membranes (5.0 mg Chl/mL) suspended in a pH 6.0 Mes buffer (10 mM Mes and 5 mM NaCl) was mixed with 1.0 μL of 200 mM sodium formate, 1 μL of 20 mM potassium ferricyanide, and 1 μL of 20 mM potassium ferrocyanide. The sample was dried on a CaF_2 plate under N_2 gas flow to make a film (6 mm in diameter), which was then sealed with another CaF_2 plate with a greased Teflon spacer (1.0 mm in thickness). The dry film was hydrated by placing 2 μL of 40% (v/v) glycerol/H_2O in a sealed infrared cell without touching the sample (*34*). For replacement of unlabeled H_2O with $H_2{}^{18}O$ (Euriso-top, 95.4 at. % ^{18}O) [or D_2O (Aldrich, 99.9 at % D)], the film was dried and hydrated (deuterated) by placing 2 μL of $H_2{}^{18}O$ (D_2O) in the sealed cell. This procedure was repeated 4 times at intervals of 10 min, and 2 μL of 40% (v/v) glycerol/$H_2{}^{18}O$ [glycerol$(OD)_3$ (CDN, 98.7 at % D)/D_2O] was placed for final hydration (deuteration). The sample temperature was adjusted to 10 °C by circulating cold water in a copper holder. The sample was stabilized at this temperature in the dark for more than 1 h before the measurements were begun.

Flash-induced FTIR spectra were recorded on a Brucker IFS-66/S spectrophotometer equipped with an MCT detector (D313-L). Flash illumination was performed using a Q-switched Nd:YAG laser (INDI-40-10; 532 nm; ~7 ns fwhm; 9 mJ $pulse^{-1}$ cm^{-2}). Single-beam spectra with 100 scans (50 s accumulation) were recorded before and after five flash illuminations (1 Hz). The measurement was repeated with dark relaxation for 750 s between measurements. The spectra of 18, 30, and 150 cycles were averaged for *T. elongatus* PSII with formate, that without formate, and spinach PSII, respectively, to calculate a $Y_D^{\bullet}/Y_D$ difference spectrum as after-minus-before illumination.

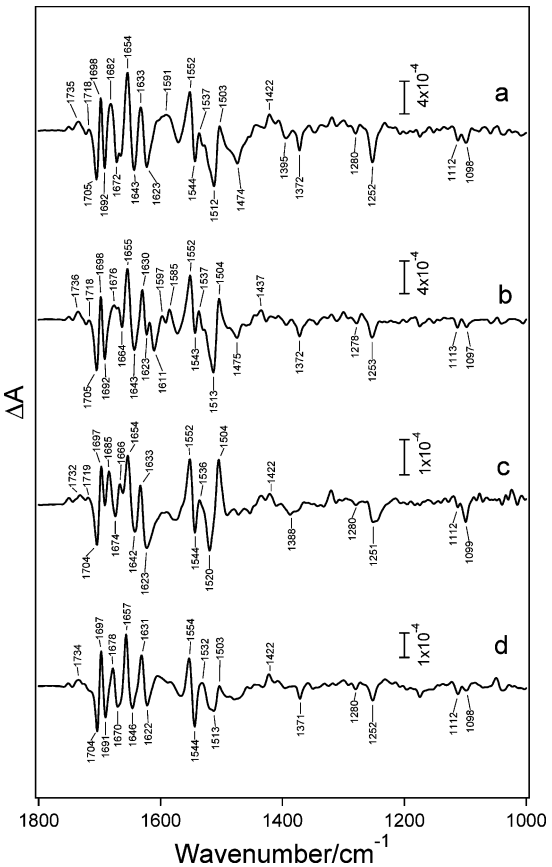

FIGURE 1: Light-induced $Y_D^{\bullet}/Y_D$ FTIR difference spectra in the mid-frequency region (1800−1000 cm^{-1}) obtained using moderately hydrated or deuterated films of Mn-depleted PSII preparations in Mes buffers at pH 6.0. (a) Hydrated PSII core complexes from *T. elongatus*. (b) Deuterated PSII core complexes from *T. elongatus*. (c) Hydrated PSII core complexes from *T. elongatus* in the absence of formate. (d) Hydrated PSII membranes from spinach. Samples other than for panel c contained formate to prevent contamination of non-heme iron signals. The sample temperature was adjusted to 10 °C.

RESULTS

Figure 1a shows a $Y_D^{\bullet}/Y_D$ FTIR difference spectrum in the mid-frequency region (1800−1000 cm^{-1}) obtained using a moderately hydrated film of Mn-depleted PSII core complexes from *T. elongatus*. The positive and negative signals correspond to $Y_D^{\bullet}$ and Y_D, respectively. The PSII sample contained formate to prevent peroxidation of non-heme iron, whose signals otherwise contaminate the $Y_D^{\bullet}/Y_D$ spectrum (*23*, *25*). Spectral features were virtually identical to previous $Y_D^{\bullet}/Y_D$ spectra of PSII core complexes from *Synechocystis* sp. PCC6803 (*22*, *23*, *26*, *27*). A positive peak at 1503 cm^{-1} and a negative peak at 1252 cm^{-1} have been assigned to the CO vibration of $Y_D^{\bullet}$ and the COH vibration of Y_D, respectively, using specific isotope labeling of Tyr residues (*22*, *26*). These frequencies are consistent with hydrogen bond interactions of $Y_D^{\bullet}$ and Y_D (*4*, *22*). The complex structure in the 1700−1600 cm^{-1} region includes

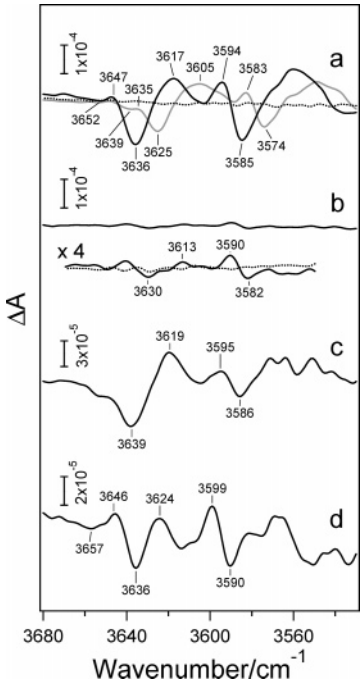

FIGURE 2: High-frequency OH stretching region (3680−3530 cm^{-1}) of the $Y_D^{\bullet}/Y_D$ FTIR difference spectra. (a) PSII core complexes from *T. elongatus* hydrated by unlabeled H_2O (black line) and $H_2{}^{18}O$ (gray line). A dark-minus-dark spectrum (dotted line) is also shown to express a noise level. (b) Deuterated PSII core complexes from *T. elongatus*. An expanded (×4) spectrum (solid line) is also shown with a dark-minus-dark spectrum (dotted line). (c) Hydrated PSII core complexes from *T. elongatus* in the absence of formate. (d) Hydrated PSII membranes from spinach. See Figure 1 caption for other conditions.

amide I bands (C═O stretch of backbone amide) due to protein conformational changes upon $Y_D^{\bullet}$ formation, while the characteristic differential signal at 1705/1698 cm^{-1} might arise from the electrochromic shift of the keto C═O band of P680 (*22*). Bands at 1600−1510 cm^{-1} may mostly arise from the amide II vibrations (NH band + CN stretch of backbone amide), and the negative peak at 1512 cm^{-1} includes the contribution of the CC stretching vibration (the 19 mode) of Y_D (*22*).

Figure 2a (black line) shows the high-frequency region (3680−3530 cm^{-1}) of the $Y_D^{\bullet}/Y_D$ difference spectrum. This region includes the OH stretching vibrations of weakly hydrogen bonded OH groups. Two major differential signals appeared at 3636(−)/3617(+) and 3594(+)/3585(−) (+ and − indicate positive and negative intensity, respectively), along with a minor signal at 3652(−)/3647(+) cm^{-1}. Upon $H_2{}^{18}O$ substitution, the major signals downshifted by 11−12 cm^{-1} to 3625(−)/3605(+) and 3583(+)/3574(−) cm^{-1}, and the minor signal also seems to downshift to 3639(−)/3635(+) cm^{-1} (Figure 2a, gray line). The spectrum in the mid-frequency region was virtually unchanged by $H_2{}^{18}O$ substitution (data not shown).

Upon deuteration of the PSII core film, many peaks underwent frequency shifts and/or intensity changes in the 1800−1000 cm^{-1} region (Figure 1b). For example, in the amide I region, peaks at 1682(+)/1672(−) diminished and were replaced by a small signal at 1676(+)/1664(−), while the peaks at 1633(+)/1623(−)/1591(+) cm^{-1} were changed to more complex features with peaks at 1630(+)/1623(−)/1611(−)/1597(+)/1585(+) cm^{-1}. Although the present sample in a deuterated film was incubated at 10 °C only for 1−2 h before measurement, the spectrum of the sample incubated in D_2O for more than 2 days at 10 °C was virtually identical to the spectrum in Figure 1b (data not shown). Thus, exchangeable protons in the protein matrix coupled to Y_D as well as a proton of Y_D itself were fully deuterated in the procedure used in this study. Previous EPR experiments showed that the half time of H/D exchange of the Y_D proton is 9 h for the PSII core complexes of *Synechocystis* sp. PCC 6803 (*17*, *19*). The much faster exchange rate observed in the present experiment can be ascribed to several reasons such as repetitive light reactions during FTIR measurement, incubation at 10 °C, the presence of formate, and the difference in species (*T. elongatus* vs *Synechocystis* sp. PCC 6803).

In the high-frequency region, the OH signals observed in the hydrated PSII film almost disappeared upon deuteration (Figure 2b). Expansion of the spectrum (Figure 2b, lower spectrum, solid line), however, showed that very small peaks remain at 3630(−)/3613(+) and 3590(+)/3582(−) cm^{-1} (the noise level is shown with a dotted line in Figure 2b). These small peaks originate from residual protons in the deuterated sample and hence most probably arise from the OH vibrations of HOD species. The peak positions downshifted by 3−6 cm^{-1} from the original peaks at 3636(−)/3617(+) and 3594(+)/3585(−) cm^{-1} in the hydrated sample (Figure 2a, black line). It is noted that measurement in an H_2O/D_2O (1:1) mixture showed the peaks from both H_2O and HOD with comparable intensities (data not shown), confirming this interpretation.

The samples for Figures 1a,b and 2a,b contained formate. Hienerwadel et al. (*23*) reported that formate is coupled with Y_D through a hydrogen bond network, although the hydrogen bond interaction of Y_D itself is unaffected. To study the effect of formate on the OH signals, we measured a $Y_D^{\bullet}/Y_D$ spectrum with the PSII core sample in the absence of formate (Figures 1c and 2c). Although the spectrum was slightly contaminated with non-heme iron signals as typically seen by a negative peak at 1099 cm^{-1} arising from the His ligands of the non-heme iron (Figure 1c) (*35*, *36*), the effect of the absence of formate was basically identical to the previous measurement (*23*); a negative peak at 1692 cm^{-1} diminished, and a new signal appeared at 1674(−)/1666(+) cm^{-1}. The high-frequency OH region showed peaks at 3639(−)/3619(+) and 3595(+)/3586(−) cm^{-1} (Figure 2c). These signals were very similar to those at 3636/3617 and 3594/3585 cm^{-1} in the presence of formate (Figure 2a), although the peak positions upshifted by 1−3 cm^{-1} and the relative intensities of the signals were slightly altered.

Figures 1d and 2d show the $Y_D^{\bullet}/Y_D$ spectrum in the mid- and high-frequency regions, respectively, of the Mn-depleted PSII membranes of spinach in the presence of formate. The mid-frequency spectrum (Figure 1d) is basically in agreement with the previous spectrum of spinach PSII membranes (*25*). Notably, peak positions of CO (1503 cm^{-1}) and COH (1252 cm^{-1}) vibrations by $Y_D^{\bullet}$ and Y_D, respectively, were identical between *T. elongatus* and spinach (Figure 1a,d). In the OH stretching region (Figure 2d), signals were observed at 3657(−)/3646(+), 3636(−)/3624(+), and 3599(+)/3590(−) cm^{-1}. These signals were similar to those of *T. elongatus* (Figure 2a, black line), although the peak frequencies differ by −1 to +7 cm^{-1}.

DISCUSSION

The $Y_D^{\bullet}/Y_D$ spectrum of Mn-depleted PSII core complexes of *T. elongatus* showed prominent differential signals at 3636(−)/3617(+) and 3594(+)/3585(−) cm^{-1} in the OH stretching region (Figure 2a, black line). These signals downshifted by 11−12 cm^{-1} upon $H_2{}^{18}O$ substitution (Figure 1a, gray line) and almost disappeared upon deuteration (Figure 2b). Thus, these bands were definitely assigned to the OH stretching vibrations of water molecule(s). This frequency region is typical of weakly hydrogen bonded OH vibrations (*28*−*31*), while strongly hydrogen bonded OH vibrations occur at lower frequencies (<3500 cm^{-1}) but with broad widths (*37*). Such broad features along with superimposition of the NH stretching bands of protein backbones hamper identification of strongly H-bonded OH bands.

If a H_2O molecule has a symmetric hydrogen bond structure, two OH vibrations couple with each other and split into asymmetric and symmetric stretching vibrations. For example, in water vapor, in which both OH bonds are free from a hydrogen bond, asymmetric and symmetric OH vibrations take place at 3756 and 3657 cm^{-1}, respectively, as a result of the intermolecular coupling of ∼50 cm^{-1} (*38*). In the $Y_D^{\bullet}/Y_D$ spectrum, the couplings were estimated to be only 3−6 cm^{-1} from the frequencies of residual HOD in a deuterated PSII sample (Figure 2b, expanded spectrum). These small coupling values indicate that the water molecules detected in the present study have highly asymmetric hydrogen bond interactions (i.e., one is weakly hydrogen bonded and the other is strongly hydrogen bonded). This observation also indicates that the two differential signals at 3636/3617 and 3594/3585 cm^{-1} arise from weakly hydrogen bonded OH bonds of two different water molecules.

Thus, it is concluded that at least two water molecules are structurally coupled to Y_D and that they change their interactions upon Y_D oxidation. The downshift from 3636 to 3617 cm^{-1} and the upshift from 3594 to 3585 cm^{-1} upon $Y_D^{\bullet}$ formation imply that the hydrogen bond interaction of one water is strengthened and that of the other water is weakened. The presence of these water molecules and interaction changes upon $Y_D^{\bullet}$ formation were basically unchanged whether the sample involves formate or not (Figure 2a,c). The slight changes in frequencies (by 1−3 cm^{-1}) and relative intensities are consistent with the binding of formate in the hydrogen bond network (*23*), although the possibility that water bands in contaminating non-heme iron signals contribute to these changes cannot be excluded at present. Similar water bands were also observed at 3636(−)/3624(+) and 3599(+)/3590(−) cm^{-1} in the $Y_D^{\bullet}/Y_D$ spectrum of Mn-depleted PSII membranes of spinach (Figure 2d). Thus, these two water molecules commonly exist near Y_D irrespective of species. In addition, the third water molecule that is weakly coupled to Y_D may exist to show a weak signal at 3652(−)/3647(+) cm^{-1} in *T. elongatus* and at 3657(−)/3646(+) cm^{-1} in spinach (Figure 2a,d).

These water molecules are probably involved in a hydrogen bond network around the phenolic OH of Y_D. The previous ENDOR study showed that three or fewer protons are located within a shell between 4.5 and 8.5 Å (*18*). Some of these protons may arise from the water molecules observed in the FTIR spectra. An exchangeable proton hydrogen bonded to $Y_D^{\bullet}$ has been detected by ENDOR and ESEEM measurements (*13*−*19*). This proton is most probably attributed to D2-H189 interacting with $Y_D^{\bullet}$ (*17*, *20*−*22*). Notably, the ESEEM study by Diner et al. (*19*) showed the presence of another hydrogen bonded proton in *Synechocystis* PSII. According to the X-ray structures (*11*, *12*), another neighboring amino acid D2-Gln164 is located at a weak hydrogen bond distance of 3.1−3.5 Å (between nitrogen or oxygen of the Gln side chain and the Y_D oxygen) but with an orientation inappropriate to hydrogen bonding [the C−O···N(O) angle is 67−68°, and the dihedral angle formed between benzene plane and C−O···N(O) is 73−89°]. Thus, it may be possible that a water molecule is another hydrogen bond partner directly interacting with Y_D. Although the ESEEM result suggested only one hydrogen bond in spinach $Y_D^{\bullet}$ (*19*), FTIR spectra showed that the CO (1503 cm^{-1}) and COH (1252 cm^{-1}) vibrations of $Y_D^{\bullet}$ and Y_D, respectively, are virtually identical between cyanobacteria (*T. elongatus* and *Synechocystis* sp. PCC 6803) and spinach (Figure 1a,d) (*22*, *25*, *26*), indicating that the hydrogen bond interactions of Y_D are conserved among species. It should be noted that the H-bond network around Y_D could be slightly modified in Mn-depleted PSII. However, because a significant change in the Y_D property upon Mn depletion has not been reported, it is highly likely that the immediate H-bond environment of Y_D remains intact even after Mn depletion.

The proton released from Y_D upon its oxidation may remain in the vicinity of Y_D (*2*, *3*, *23*) or may be partly released from the protein (*23*). Water molecules around Y_D may form a proton-transfer pathway by connecting polar residues. A high dielectric property of water can stabilize the positive charge produced in the vicinity of Y_D and thus could contribute to its low redox potential [+0.72−0.76 mV (*8*, *9*) vs approximately +1 V of $Y_Z^{\bullet}/Y_Z$ (*1*)]. In addition, if a water molecule is a hydrogen bond partner to Y_D, this water can be directly involved in the Y_D reaction by such as tuning the redox potential through a hydrogen bond interaction and accepting a proton immediately from Y_D. Thus, water molecules coupled to Y_D may play crucial roles in the molecular mechanism of the proton-coupled electron-transfer reaction of Y_D.

REFERENCES

1. Diner, B. A., and Babcock, G. T. (1996) Structure, dynamics, and energy conversion efficiency in photosystem II, in *Oxygenic Photosynthesis: The Light Reactions* (Ort, D. R., and Yocum, C. F., Eds.) pp 213−247, Kluwer, Dordrecht, The Netherlands.
2. Diner, B. A. (2001) Amino acid residues involved in the coordination and assembly of the manganese cluster of photosystem II. Proton-coupled electron transport of the redox-active tyrosines and its relationship to water oxidation, *Biochim. Biophys. Acta 1503*, 147−163.
3. Rutherford, A. W., Boussac, A., and Faller, P. (2004) The stable tyrosyl radical in photosystem II: Why D, *Biochim. Biophys. Acta 1655*, 222−230.
4. Berthomieu, C., and Hienerwadel, R. (2005) Vibrational spectroscopy to study the properties of redox-active tyrosines in photosystem II and other proteins, *Biochim. Biophys. Acta 1707*, 51−66.
5. Diner, B. A., and Britt, R. D. (2005) The redox-active tyrosines Y_Z and Y_D, in *Photosystem II: The Light-Driven Water/Plastoquinone Oxidoreductase* (Wydrzynski, T., and Satoh, K. Eds.), Ch. 16, pp 207−233, Springer, Dordrecht, The Netherlands.
6. Dixon, W. T., and Murphy, D. (1976) Determination of the acidity constants of some phenol radical cations by means of electron spin resonance, *J. Chem. Soc., Faraday Trans. 2*, *72*, 1221−1230.

7. Sugiura, M., Rappaport, F., Brettel, K., Noguchi, T., Rutherford, A. W., and Boussac, A. (2004) Site-directed mutagenesis of *Thermosynechococcus elongatus* photosystem II: The O_2 evolving enzyme lacking the redox active tyrosine D, *Biochemistry 43*, 13549−13563.
8. Boussac, A., and Etienne, A. L. (1984) Midpoint potential of signal II (slow) in Tris-washed photosystem-II particles, *Biochim. Biophys. Acta 766*, 576−581.
9. Vass, I., and Styring, S. (1991) pH-Dependent charge equilibria between tyrosine D and the S states in photosystem II. Estimation of relative midpoint redox potentials, *Biochemistry 30*, 830−839.
10. Ishikita, H., and Knapp, E. W. (2006) Function of redox-active tyrosine in photosystem II, *Biophys. J. 90*, 3886−3896.
11. Ferreira, K. N., Iverson, T. M., Maghlaoui, K., Barber, J., and Iwata, S. (2004) Architecture of the photosynthetic oxygen-evolving center, *Science (Washington, DC, U.S.) 19*, 1831−1838.
12. Loll, B., Kern, J., Saenger, W., Zouni, A., and Biesiadka, J. (2005) Towards complete cofactor arrangement in the 3.0 Å resolution structure of photosystem II, *Nature (London, U.K.) 7070*, 1040−1044.
13. Rodriguez, I. D., Chandrashekar, T. K., and Babcock, G. T. (1987) ENDOR characterization of H_2O/D_2O exchange in the D^+Z^+ radical in photosynthesis, in *Progress in Photosynthesis* (Biggins, J., Ed.) Vol. 1, pp 471−474, Martinus Nijhoff Publishers, Dordrecht, The Netherlands.
14. Evelo, R. G., Hoff, A. J., Dikanov, S. A., and Tyryshkin, A. M. (1989) An ESEEM study of the oxidized electron donor of plant photosystem II: Evidence that D is a neutral tyrosine radical, *Chem. Phys. Lett. 161*, 479−484.
15. Mino, H., Satoh, J., Kawamori, A., Toriyama, K., and Zimmermann, J.-L. (1993) Matrix ENDOR of tyrosine D^+ in oriented photosystem II membranes, *Biochim. Biophys. Acta 1144*, 426−433.
16. Force, D. A., Randall, D. W., Britt, R. D., Tang, X.-S., and Diner, B. A. (1995) ^{2}H ESE-ENDOR study of hydrogen bonding to the tyrosine radicals $Y_D^\bullet$ and $Y_Z^\bullet$ of photosystem II, *J. Am. Chem. Soc. 117*, 12643−12644.
17. Tang, X.-S., Chisholm, D. A., Dismukes, G. C., Brudvig, G. W., and Diner, B. A. (1993) Spectroscopic evidence from site-directed mutants of *Synechocystis* PCC6803 in favor of a close interaction between histidine 189 and redox-active tyrosine 160, both of polypeptide D2 of the photosystem II reaction center, *Biochemistry 32*, 13742−13748.
18. Tang, X.-S., Zheng, M., Chisholm, D. A., Dismukes, G. C., and Diner, B. A. (1996) Investigation of the differences in the local protein environments surrounding tyrosine radicals $Y_Z^\bullet$ and $Y_D^\bullet$ in photosystem II using wild-type and the D2-Tyr160Phe mutant of *Synechocystis 6803*, *Biochemistry 35*, 1475−1484.
19. Diner, B. A., Force, D. A., Randall, D. W., and Britt, R. D. (1998) Hydrogen bonding, solvent exchange, and coupled proton and electron transfer in the oxidation and reduction of redox-active tyrosine Y_Z in Mn-depleted core complexes of photosystem II, *Biochemistry 37*, 17931−17943.
20. Campbell, K. A., Peloquin, J. M., Diner, B. A., Tang, X.-S., Chisholm, D. A., and Britt, R. D. (1997) The τ-nitrogen of D2 histidine 189 is the hydrogen bond donor to the tyrosine radical Y_D of photosystem II, *J. Am. Chem. Soc. 119*, 4787−4788.
21. Un, S., Boussac, A., and Sugiura, M. (2007) Characterization of the tyrosine-Z radical and its environment in the spin-coupled S_2-$Tyr_Z^\bullet$ state of photosystem II from *Thermosynechococcus elongatus*, *Biochemistry 46*, 3138−3150.
22. Hienerwadel, R., Boussac, A., Breton, J., Diner, B. A., and Berthomieu, C. (1997) Fourier transform infrared difference spectroscopy of photosystem II tyrosine D using site-directed mutagenesis and specific isotope labeling, *Biochemistry 36*, 14712−14723.
23. Hienerwadel, R., Gourion-Arsiquaud, S., Ballottari, M., Bassi, R., Diner, B. A., and Berthomieu, C. (2005) Formate binding near the redox-active tyrosine D in photosystem II: Consequences on the properties of Tyr_D, *Photosynth. Res. 84*, 139−144.
24. Noguchi, T., and Berthomieu, C. (2005) Molecular analysis by vibrational spectroscopy, in *Photosystem II: The Light-Driven Water/Plastoquinone Oxidoreductase* (Wydrzynski, T., and Satoh, K. Eds.), Ch. 16, pp 367−387, Springer, Dordrecht, The Netherlands.
25. Hienerwadel, R., Boussac, A., Breton, J., and Berthomieu, C. (1996) Fourier transform infrared difference study of tyrosine D oxidation and plastoquinone Q_A reduction in photosystem II, *Biochemistry 35*, 15447−15460.
26. Noguchi, T., Inoue, Y., and Tang, X.-S. (1997) Structural coupling between the oxygen-evolving Mn cluster and a tyrosine residue in photosystem II as revealed by Fourier transform infrared spectroscopy, *Biochemistry 36*, 14705−14711.
27. Chu, H. A., Hillier, W., and Debus, R. J. (2004) Evidence that the C-terminus of the D1 polypeptide of photosystem II is ligated to the manganese ion that undergoes oxidation during the S_1 to S_2 transition: An isotope-edited FTIR study, *Biochemistry 43*, 3152−3166.
28. Maeda, A., Kandori, H., Yamazaki, Y., Nishimura, S., Hatanaka, M., Chon, Y.-S., Sasaki, J., Needleman, R., and Lanyi, J. K. (1997) Intramembrane signaling mediated by hydrogen-bonding of water and carboxyl groups in bacteriorhodopsin and rhodopsin, *J. Biochem. 121*, 399−406.
29. Kandori, H. (2000) Role of internal water molecules in bacteriorhodopsin, *Biochim. Biophys. Acta 1460*, 177−191.
30. Noguchi, T., and Sugiura, M. (2000) Structure of an active water molecule in the water oxidizing complex of photosystem II as studied by FTIR spectroscopy, *Biochemistry 39*, 10943−10949.
31. Noguchi, T., and Sugiura, M. (2002) FTIR detection of water reactions during the flash-induced S-state cycle of the photosynthetic water-oxidizing complex, *Biochemistry 41*, 15706−15712.
32. Sugiura, M., and Inoue, Y. (1999) Highly purified thermo-stable oxygen-evolving photosystem II core complex from the thermophilic cyanobacterium *Synechococcus elongatus* having His-tagged CP43, *Plant Cell Physiol. 40*, 1219−1231.
33. Ono, T., and Inoue, Y. (1986) Effects of removal and reconstitution of the extrinsic 33, 24, and 16 kDa proteins on flash oxygen yield in photosystem II particles, *Biochim. Biophys. Acta 850*, 380−389.
34. Noguchi, T., and Sugiura, M. (2002) Difference spectra of the water oxidizing complex in moderately hydrated photosystem II core films: Effect of hydration extent on S-state transitions, *Biochemistry 41*, 2322−2330.
35. Hienerwadel, R., and Berthomieu, C. (1995) Bicarbonate binding to the non-heme iron of photosystem II investigated by FTIR difference spectroscopy and ^{13}C-labeled bicarbonate, *Biochemistry 34*, 16288−16297.
36. Noguchi, T., and Inoue, Y. (1995) Identification of FTIR signals from the non-heme iron in photosystem II, *J. Biochem. 118*, 9−12.
37. Luck, W. A. P., Klein, D., and Rangsriwatananon, K. (1997) Anticooperativity of the two water OH groups, *J. Mol. Struct. 416*, 287−296.
38. Benedict, W. S., Gailar, N., and Plyler, E. K. (1956) Rotation−vibration spectra of deuterated water vapor, *J. Chem. Phys. 24*, 1139−1165.

BI701752D